BMC Cancer

RESEARCH

Open Access

The co-location of MARCO + macrophages and SPOCK1 + fibroblasts contributes to the poor prognosis and undesirable immunotherapy response in colorectal cancer

Yuhao Pan[1], Hao Ying[1], Meiyin Luo[2] and Qijia Xuan[1*]

Abstract

Intratumor macrophage infiltration plays a crucial role in various aspects of tumor immunity in colorectal cancer (CRC). However, the phenotypic heterogeneity, spatial distribution, and cellular interactions of these macrophages remain elusive. To overcome the limitations, bulk, single-cell, and spatial transcriptomics were utilized synergistically. We identified two distinct spatial patterns of macrophage infiltration: macrophage + and macrophage-. MARCO + macrophages were found to accumulate intratumorally in the macrophage + infiltration. Notably, bulk and spatial transcriptomics data revealed a consistent co-location of MARCO + macrophages with SPOCK1 + fibroblasts, which was further validated by multiplex immunofluorescence. The co-location of MARCO + macrophages and SPOCK1 + fibroblasts was associated with poor prognosis and undesirable immunotherapy response in CRC. MARCO + macrophages and SPOCK1 + fibroblasts collectively established an immunosuppressive tumor microenvironment. MARCO + macrophages promoted the proliferation of SPOCK1 + fibroblasts via SPP1 and EGF signaling pathways. Meanwhile, SPOCK1 + fibroblasts contributed to the M2 polarization of MARCO + macrophages through the C3-C3AR1 axis. Our findings suggest that targeting MARCO + macrophages, SPOCK1 + fibroblasts, or their interaction could represent a promising therapeutic strategy for CRC.

Keywords MARCO, SPOCK1, Colorectal cancer, Tumor microenvironment, Macrophage, Fibroblast

Introduction

Colorectal cancer (CRC) is the third most commonly diagnosed malignancy and the second leading cause of cancer-related mortality worldwide [1]. Although immunotherapy, with rapid development, has emerged as a promising treatment for various cancers, its efficacy in CRC remains limited [2]. Only a small subset of metastatic CRC patients (approximately 5%) with mismatch repair deficiency and high microsatellite instability (MSI-H) benefit from anti-PD-1 therapy [3, 4]. Thus, there is an urgent need to explore the factors that contribute to the immunosuppressive tumor microenvironment (TME)

*Correspondence:
Qijia Xuan
xuanqijia@zju.edu.cn
[1]Department of Oncology, the Fourth Affiliated Hospital of School of Medicine, and International School of Medicine, International Institutes of Medicine, Zhejiang University, Yiwu 322000, China
[2]The Department of Otolaryngology Head and Neck Surgery, Sir Run Run Shaw Hospital, Affiliated to Zhejiang University School of Medicine, Hangzhou, China

in CRC, which could reveal new targets for improving immunotherapy outcomes.

Macrophages are crucial regulators of the TME and play diverse roles in tumor immunity [5]. Traditionally, macrophages can polarize into two types, namely M1 or M2 macrophages [6]. The M1 phenotype is characterized by pro-inflammatory properties, while the M2 phenotype features anti-inflammatory properties [7]. However, for macrophages accumulating in tumor tissues, recognized as tumor-associated macrophages (TAMs), there is great heterogeneity and complex phenotypes [8]. For instance, FABP5 + lipid-loaded macrophages suppress T-cell-mediated anti-tumor immunity in hepatocellular carcinoma by processing unsaturated fatty acids from tumor cells [9]. NRF2-activated macrophages promote cancer invasiveness and metastatic potential by stabilizing epithelial-mesenchymal transition in CRC [10]. Within the TME, macrophages interact with other cells, such as fibroblasts, to influence tumor progression. In gastric cancer, CCL2 + fibroblasts and STAT3-activated macrophages collaborate to create an immunosuppressive TME and drive tumor growth [11]. Similarly, crosstalk between FAP + fibroblasts and SPP1 + macrophages is associated with CRC progression and resistance to immunotherapy [12]. Beyond cellular heterogeneity, the spatial distribution (intratumoral and stromal) of TME components, is linked to the clinical outcomes of cancer patients [13, 14]. Nevertheless, the spatial patterns of intratumor macrophage infiltration and their interactions with other cells in CRC are not fully elucidated.

Bulk transcriptomics data provides a combined expression profile of distinct cell types in the specific tissue. Single-cell RNA sequencing resolves gene expression heterogeneity at the individual cell level, uncovering complex cellular interactions within the TME [15, 16]. The development of spatial transcriptomics (ST) technology makes it possible to obtain the spatial location of genes, allowing for the detailed capture of the molecular and cellular characteristics of the TME [17]. Integrating bulk, single-cell, and spatial transcriptomics data can thus provide a comprehensive understanding of cellular heterogeneity, cell–cell communication, and spatial organization in the CRC TME.

In this study, we utilized ST to investigate the intratumor macrophage infiltration patterns in CRC, which was delineated as macrophage + and macrophage-. Notably, MARCO + macrophages accumulated intratumorally in the macrophage + sample. Furthermore, SPOCK1 + fibroblasts were consistently co-localized with MARCO + macrophages in both bulk transcriptomics and ST data, a finding confirmed by multiplex immunofluorescence (MIF) in 30 CRC samples. MARCO + macrophages and SPOCK1 + fibroblasts collectively shaped an immunosuppressive TME. The co-existence of MARCO + macrophages and SPOCK1 + fibroblasts was linked to worse survival and immunotherapy response. Together, our study provides new insights into intratumor macrophage infiltration in CRC and highlights the co-location of MARCO + macrophages and SPOCK1 + fibroblasts as a key determinant of immune suppression.

Materials and methods

Data collection

The ST data of three CRC samples was collected from the study by Sibai et al. [18]. Two CRC single-cell datasets, GSE205506 (17 tumor samples) and GSE132465 (23 tumor samples), were obtained from the Gene Expression Omnibus (GEO) database (https://www.ncbi.nlm.nih.gov/geo/), and the corresponding clinical data were obtained from the original studies [19, 20]. The GSE205506 dataset contained CRC patients who underwent immunotherapy, with pathological complete response (pCR) and non-pCR distinguished according to the treatment outcomes. The bulk transcriptomics data of 591 CRC samples and relevant clinical information were downloaded from the Cancer Genome Atlas (TCGA) database (https://portal.gdc.cancer.gov/). The unit for bulk expression data was log(TPM + 1), while ST or single-cell data was UMI count. The summary of all the data used in this study was shown in Table S1.

Patient samples

Formalin-fixed paraffin-embedded (FFPE) tissues were collected from 30 patients with CRC at the Fourth Affiliated Hospital of School of Medicine, Zhejiang University. The study was approved by the Ethics Committee of the Fourth Affiliated Hospital of School of Medicine, Zhejiang University (No: K2025019) and was in compliance with the Declaration of Helsinki. Informed written consent from all patients involved was obtained.

Analysis of ST data

The ST data were analyzed using the R package SpaCET [21]. The SpaCET.quality.control function was utilized to filter out spots with low gene detection. We assessed the abundance of malignant cells using the SpaCET.identify.interface function. The SpaCET.GeneSetScore function was used to calculate the score of gene sets in each spot. We employed the SpaCET.visualize.spatialFeature function to visualize the findings.

Single-cell data preprocessing

The R package Seurat was used for the analysis of single-cell data. Cells expressing more than 300 genes, with the ratio of mitochondrial genes less than 30% and ribosomal genes less than 50%, were retained. The top 2000 most variable genes were selected for the principal component

analysis. The R package Harmony was utilized for batch effect correction within the dataset. We performed the clustering analysis using the FindNeighbors and FindClusters functions of the R package Seurat. Cells were annotated based on classical cell markers, including epithelial cells (EPCAM, KRT8, KRT18), fibroblasts (DCN, COL1A1, ACTA2), endothelial cells (PLVAP, VWF, PECAM1), T cells (CD3D, CD3E, TRAC), B cells (MS4A1, CD79A, CD79B), myeloid cells (CD14, CD68, FCGR3A), and plasma cells (JCHAIN, MZB1). The AggregateExpression function of the R package Seurat was used to obtain the pseudo-bulk expression matrix of specific cells.

Differential expression analysis and gene set enrichment analysis

The FindMarkers function of the R package was used to identify differentially expressed genes (DEGs) between two groups at the single-cell and ST level (logfc.threshold = 0.25 and min.pct = 0.1). In the bulk transcriptomics data, the R package limma was utilized to screen DEGs between two groups. We used the R package fgsea to perform gene set enrichment analysis (GSEA) to assess the enrichment of hallmark pathways based on identified DEGs.

MIF

Co-staining of two antigens was performed using a Four color mIHC Fluorescence kit (Recordbio Biological Technology, Shanghai, China) based on the tyramide signal amplification (TSA) technology according to the manufacture's instruction. Paraffin sections of tumor tissues were first subjected to dewaxing, antigen recovery, and antigen blocking, followed by incubation with primary antibodies overnight at 4 °C. After washing three times, the sections were incubated with secondary antibody from the mIHC Fluorescence kit for 50 min at room temperature, followed by the corresponding fluorescent dyes for 4 min at room temperature. Subsequently, the sections were stained with DAPI for 5 min at room temperature and then photographed using a microscope. Primary antibodies: MARCO (abcam, ab314646), CD163 (abcam, ab182422), DCN (abcam, ab277636), SPOCK1 (Proteintech, 28203–1-AP).

Survival analysis

We used the survival R package to perform survival analysis. Survival curves were generated using the Kaplan–Meier (KM) method and the statistical significance was evaluated based on the log-rank test. High and low groups divided in the survival analysis were determined using the surv_cutpoint function of the R package survminer.

Prediction of immunotherapy response of CRC patients in the bulk transcriptomics data

The tumor immune dysfunction and exclusion (TIDE) algorithm (http://tide.dfci.harvard.edu/) was used to predict the immunotherapy response of CRC patients in the bulk transcriptomics data [22]. A high TIDE score suggested an undesirable immunotherapy response.

InferCNV analysis

The R package InferCNV was used to deduce large-scale copy number variations (CNVs) of cells in the single-cell data with parameters cutoff = 0.1 and cluster_by_groups = TRUE. B cells and plasma cells were selected as reference cells. We identified epithelial cells with a high level of CNVs as malignant cells.

Cell–cell communication analysis

The R package CellChat was used to infer cell–cell communication according to CellChatDB.human, a database for ligand-receptor interactions. The likelihood of communication interactions between cells was calculated based on the average expression of ligands and receptors in those cells.

Statistical analysis

The statistical analysis and visualization were performed using R software (version 4.4.1). The Mann–Whitney U test or Student's two-sided t-test was employed to evaluate the significance of the differences between the two groups. Correlations between two variables were assessed using Spearman's correlation test. The Chi-squared test was used for the analysis of categorical variables. A two-sided P-value < 0.05 was considered statistically significant.

Results

The intratumor infiltration landscape of macrophages in CRC

To investigate the intratumor macrophage infiltration patterns in CRC, we first used the R package SpaCET to identify the tumor, interface, and stroma regions in three CRC samples in the ST data, with over 4,700 spots for each sample (Fig. 1A). To evaluate the accuracy of identified tumor regions, the spatial distribution of epithelial markers, namely EPCAM, KRT8, and KRT18, was then explored. As anticipated, spots within tumor regions had higher expression levels of epithelial markers than other regions in three CRC samples, which confirmed that tumor regions were correctly divided (Fig. S1A). Next, the "Macro score" was calculated using three macrophage markers, including CD68, CD163, and CD86, to assess the mean degree of macrophage infiltration within each spot. Compared to Patient 2 (P2) and Patient 3 (P3), Patient 1 (P1) showed higher Macro scores in the

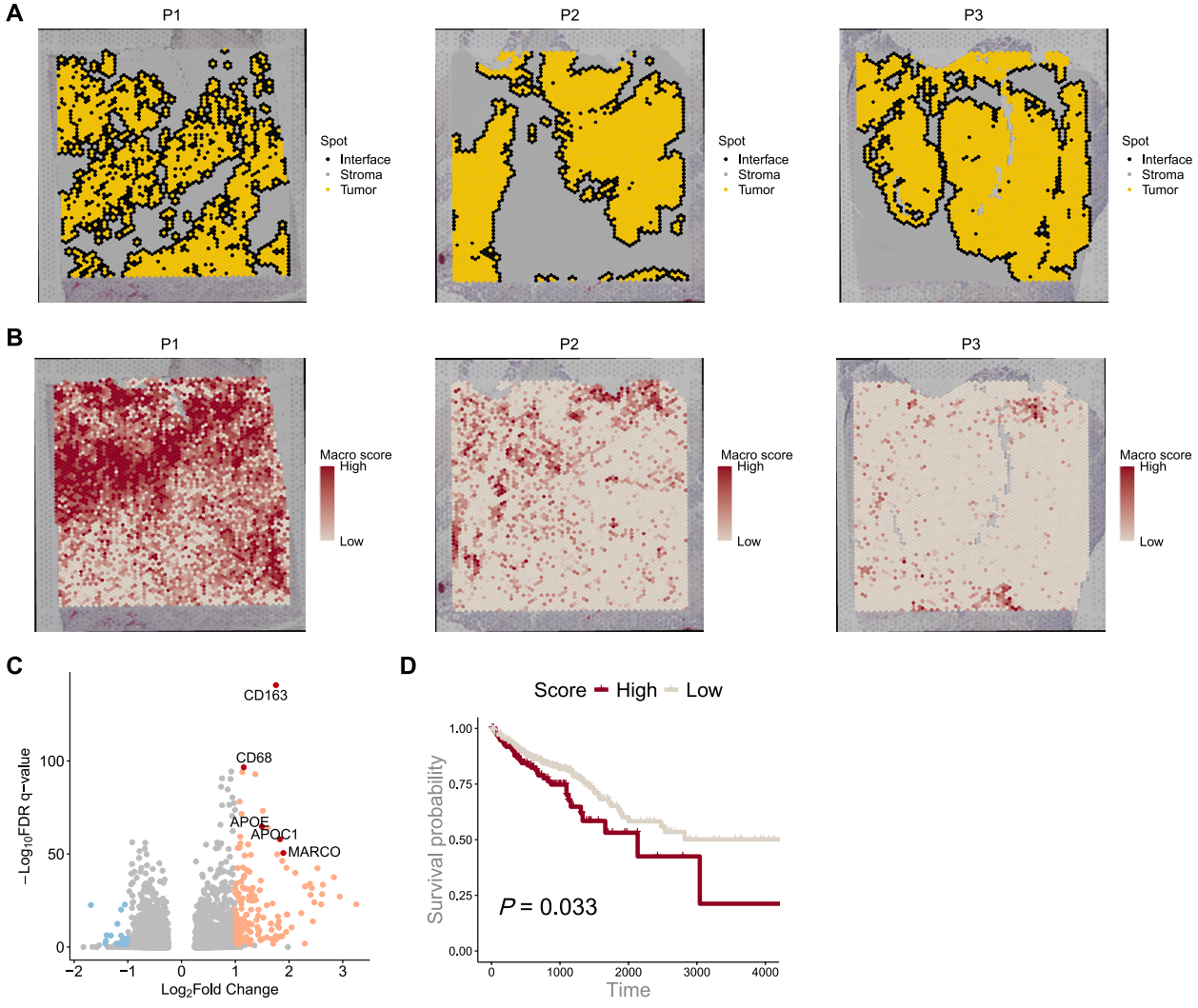

Fig. 1 The intratumor macrophage infiltration landscape in colorectal cancer (CRC). **A** The identification of tumor, stroma, and interface regions in three CRC samples in the spatial transcriptomics (ST) data. **B** The distribution of Macro score in three CRC samples in the ST data. **C** The differentially expressed genes (DEGs) of intratumor macrophage infiltration in P1. **D** The role of intratumor macrophage infiltration of P1 in the survival of CRC patients

tumor region, indicating higher infiltration of macrophages (Fig. 1B; Fig. S1B). Thus, we defined P1 as macrophage + patient while P2 and P3 as macrophage- patients. To explore the specific composition of macrophages infiltrating in the tumor region of CRC, DEGs of intratumor macrophage infiltration in P1 were screened (Fig. 1C). We noticed that CD68 and CD163 displayed high expression in P1, indicating that M2 macrophages might be the main type of intratumor macrophage infiltration in macrophage + patients with CRC. It has been demonstrated that M2 macrophages play roles in the formation of immunosuppressive TME and progression of tumor angiogenesis [23]. Additionally, APOE and APOC1, lipid-related genes, were also observed to highly express in P1. These two genes have been found to be expressed by immunosuppressive macrophages, contributing to tumor metastasis [24]. To further assess the prognostic role of intratumor macrophage infiltration in CRC, the top 50 DEGs were selected as signatures (Table S2), which were used to calculate scores by ssGSEA methods in the TCGA dataset in the bulk transcriptomics data. We found that CRC patients with higher signature scores had shorter overall survival (OS) (Fig. 1D).

MARCO + macrophages played an immunosuppressive role in the intratumor macrophage infiltration

MARCO showed high expression in the intratumor macrophage infiltration of P1, macrophage + patient. Thus, we speculated that MARCO might be soured from macrophages in CRC. Correlation analysis was then performed. In the bulk transcriptomics data, a weak correlation (R = 0.105) was observed between MARCO and CD68 (Fig. S3A), while a strong correlation (R = 0.71) was reached between MARCO and CD163 (Fig. 2A),

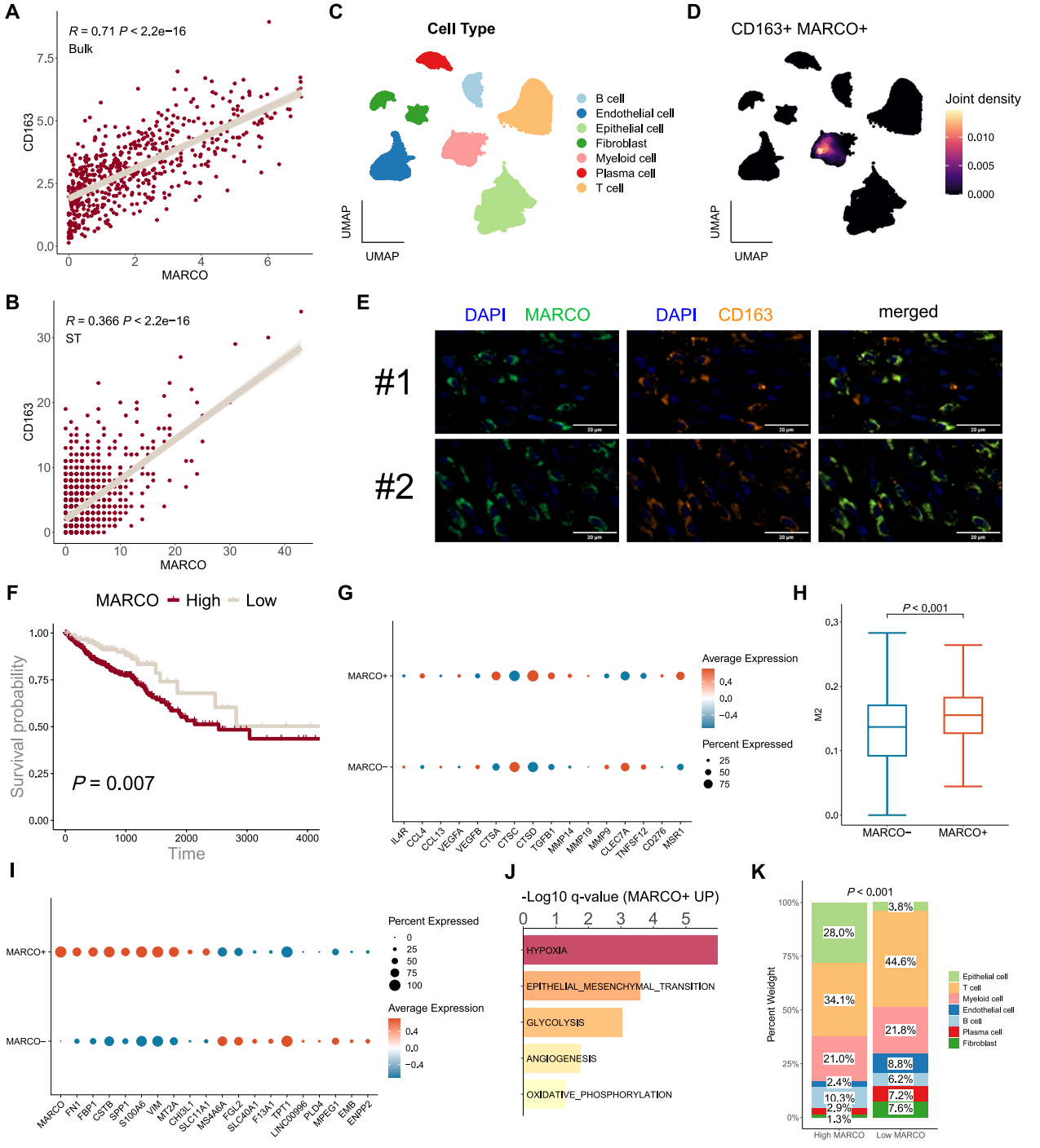

Fig. 2 MARCO + macrophages accumulated in the intratumor macrophage infiltration having an immunosuppressive impact on the tumor microenvironment (TME). **A** The correlation between MARCO and CD163 in the bulk transcriptomics data. **B** The correlation between MARCO and CD163 in the spatial transcriptomics (ST) data. **C** The single-cell dataset GSE205506 was divided into seven main clusters: B cell, endothelial cell, epithelial cell, fibroblast, myeloid cell, plasma cell, and T cell. **D** The co-expression pattern of MARCO and CD163 in the single-cell dataset GSE205506. **E** The multiplex immunofluorescence (MIF) performed on 30 patients with CRC exhibited the co-location between MARCO and CD163. **F** Colorectal cancer (CRC) patients with high MARCO expression had shorter overall survival (OS). **G** The expression differences in 18 M2 signature genes between MARCO + macrophages and MARCO- macrophages. **H** The difference in M2 score between MARCO + macrophages and MARCO- macrophages. **I** The top 10 genes upregulating in MARCO + macrophages and MARCO- macrophages. **J** The upregulated pathways in MARCO + macrophages. **K** The differences in percentages of seven main clusters (B cell, endothelial cell, epithelial cell, fibroblast, myeloid cell, plasma cell, and T cell) between CRC patients with high MARCO + macrophages and with low MARCO + macrophages in the single-cell dataset GSE205506

indicating that MARCO was a potential marker for CD163 + macrophages. We further verified the positive correlation (R = 0.366) between MARCO and CD163 in the spots of tumor region at the ST level (Fig. 2B). Subsequently, we explored the expression patterns of MARCO and CD163 at the single-cell level. After analysis of dimension reduction and clustering, seven main clusters, namely B cell, endothelial cell, epithelial cell, fibroblast, myeloid cell, plasma cell, and T cell, were identified in the single-cell dataset GSE205506, which contained a total of 55,110 cells (Fig. S2A; Fig. 2C). Co-expression of MARCO and CD163 was found in myeloid cells from the GSE205506 dataset (Fig. 2D), which was consistent with the result observed in another independent single-cell dataset, GSE132465, that included a total of 46,128 cells (Fig. S2B; Fig. S3B). At the protein level, we performed MIF analysis on 30 CRC samples and found the co-location of MARCO and CD163 (Fig. 2E; Fig. S3C). Together, MARCO was a reliable marker for CD163 + macrophages in CRC.

Survival analysis revealed that CRC patients with high MARCO expression had shorter OS, suggesting its adverse impact on clinical outcomes (Fig. 2F). Therefore, the phenotype of MARCO + macrophages in CRC was further investigated in the GSE205506 dataset. As MARCO showed a strong correlation and co-expressed with CD163, we surmised that MARCO + macrophages had M2 characteristics. We compared the expression differences in M2 signature genes between MARCO + macrophages and MARCO- macrophages [25]. Notably, TGFB1 and CD276 displayed higher expression in MARCO + macrophages, indicating immunosuppressive characteristics (Fig. 2G) [26, 27]. Additionally, MARCO + macrophages had higher M2 scores, which were calculated using the R package AUCell, than MARCO- macrophages (Fig. 2H). Hence, MARCO + macrophages could be recognized as M2 macrophages with the nature of immune inhibition in CRC. Subsequently, DEGs between MARCO + macrophages and MARCO- macrophages were screened (Fig. 2I). We noticed that FN1, FBP1, and SPP1 showed higher expression in MARCO + macrophages, which contributed to tumor progression and inhibited immune response [12, 28, 29]. Pathway analysis revealed that protumor pathways, including hypoxia and angiogenesis, were more enriched in MARCO + macrophages (Fig. 2J). Enhanced epithelial mesenchymal transition (EMT) pathway, associated with tumor metastasis, was found in MARCO + macrophages. Besides, MARCO + macrophages exhibited elevated levels of glycolysis and oxidative phosphorylation. In the bulk transcriptomics data, CRC patients with high MARCO expression also had more activation of carcinogenic and EMT pathways (Fig. S3C). Notably, TGFβ signaling pathway, linked with immunosuppression, had more enrichment in CRC patients with high MARCO expression. To explore the impact of MARCO + macrophages on TME components, we divided CRC patients with more than 200 macrophages into high and low MARCO groups based on the median proportion of MARCO + macrophages among all macrophages in the single-cell data. In the low MARCO group, a higher percentage of T cells and plasma cells with fewer epithelial cells was observed in both CRC patients treated with immunotherapy (GSE205506, Fig. 2K) and those untreated (GSE132465, Fig. S3D). Besides, pathway analysis revealed that epithelial cells of the high MARCO group showed more activation of protumor pathways (Fig. S3F). We further divided T cells into 5 subsets: CD160 + T cell, central memory T cell, effector T cell, exhausted T cell, and regulatory T cell (Fig. S3G,H). Compared to the high MARCO group, the proportion of effector T cells was a little higher in the low MARCO group (Fig. S3I).

SPOCK1 + fibroblasts accumulating in the tumor region with MARCO + macrophage infiltration contributed to the immunosuppressive TME

TME, a complex structured ecosystem, contains cancer cells, immune cells, fibroblasts, endothelial cells, and other cells. The communication and interplay between various cells of TME affect tumor progression [30]. Therefore, we further explored the differences in TME between macrophage + and macrophage- patients to uncover cell–cell interactions that could serve as promising targets for CRC immunotherapy.

DEGs of tumor regions between macrophage + and macrophage- patients were then identified. We found that markers for fibroblast, including DCN, LUM, COL1A1, COL1A2 and COL3A1, were highly expressed in P1, indicating that fibroblasts accumulated in macrophage + patients (Fig. 3A; Fig. S4A). Besides, we noticed that SPOCK1 had high expression in P1. We then investigated the spatial expression patterns of SPOCK1 in macrophage + and macrophage- patients. SPOCK1 showed significant expression in the tumor region of P1, with the distribution similar to macrophage + spots, while SPOCK1 was lowly expressed in P2 and P3 (Fig. S4B; Fig. 3B). Subsequently, the cellular source of SPOCK1 was explored. As the accumulation of fibroblasts in P1, we speculated that SPOCK1 might be a marker for fibroblasts. Correlation analysis was then performed. The correlation between SPOCK1 and DCN was 0.801 in the bulk transcriptomics data (Fig. 3C), and in intratumor spots, it was 0.365 at the ST level (Fig. 3D), suggesting that SPOCK1 was a potential marker for fibroblasts. At the single-cell level, SPOCK1 was mainly expressed in fibroblasts in the GSE205506 (Fig. 3E) and GSE132465 (Fig. S4C) datasets. At the protein level, we performed

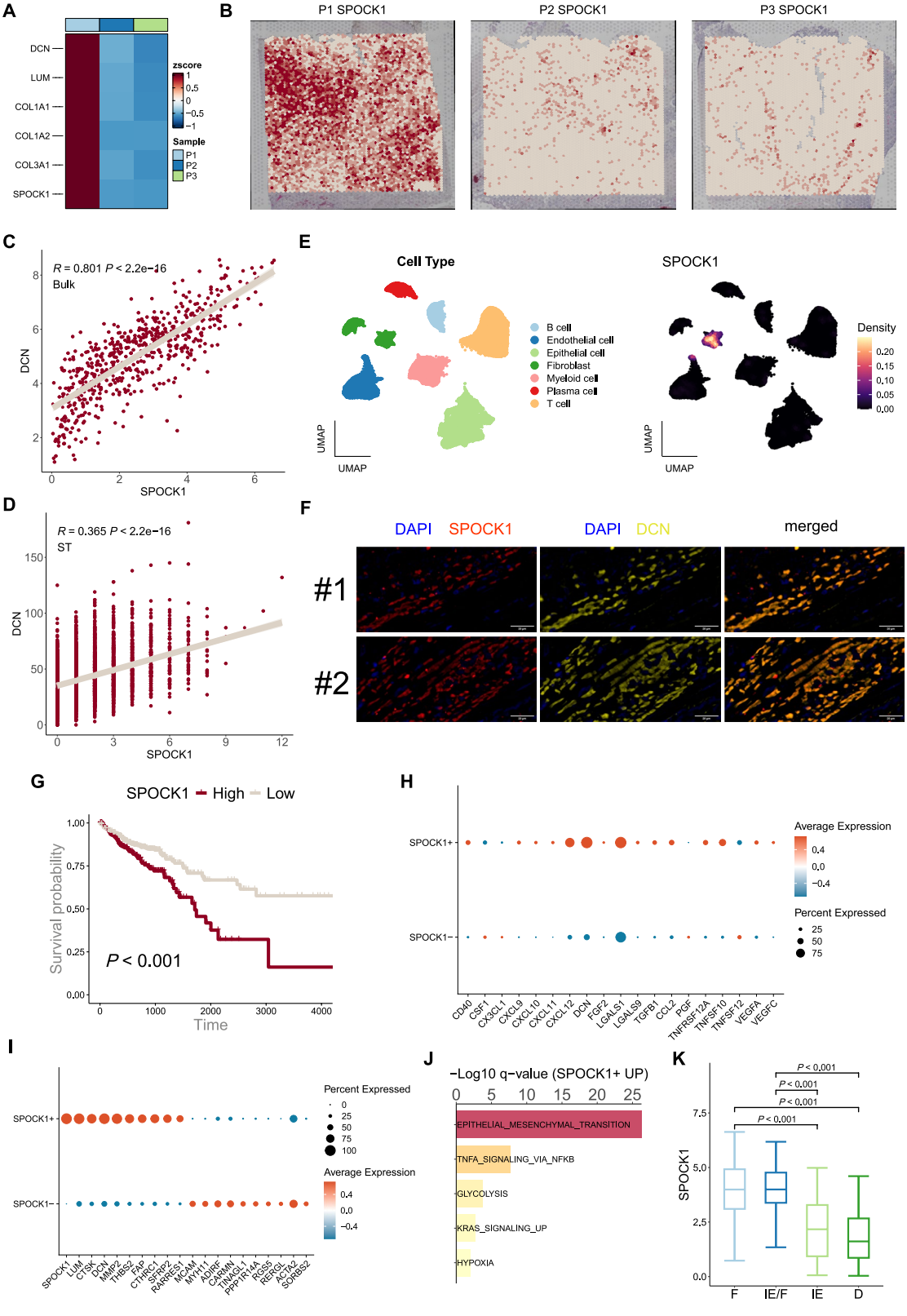

Fig. 3 (See legend on next page.)

(See figure on previous page.)

Fig. 3 SPOCK1 + fibroblasts played an immunosuppressive role in the tumor region with infiltrated MARCO + macrophages. **A** The differentially expressed genes (DEGs) of tumor regions between macrophage + and macrophage- colorectal cancer (CRC) patients. **B** The distribution of SPOCK1 in three CRC samples in the spatial transcriptomics (ST) data. **C** The correlation between SPOCK1 and DCN in the bulk transcriptomics data. **D** The correlation between SPOCK1 and DCN in the ST data. **E** The expression pattern of SPOCK1 in seven main clusters: B cell, endothelial cell, epithelial cell, fibroblast, myeloid cell, plasma cell, and T cell in the single-cell dataset GSE205506. **F** The multiplex immunofluorescence (MIF) performed on 30 patients with CRC exhibited the co-location between SPOCK1 and DCN. **G** CRC patients with high SPOCK1 expression had shorter overall survival (OS). **H** The distribution of 19 proteins from the OLINK immuno-oncology assay in SPOCK1 + fibroblasts and SPOCK1- fibroblasts. **I** The top 10 genes upregulating in SPOCK1 + fibroblasts and SPOCK1- fibroblasts. **J** The upregulated pathways in SPOCK1 + fibroblasts. **K** The differences in SPOCK1 expression among four tumor microenvironment (TME) subtypes

MIF analysis on 30 CRC samples and found the co-location of SPOCK1 and DCN (Fig. 3F; Fig. S4D). These results indicated that SPOCK1 was a dependable marker for fibroblasts.

Survival analysis revealed that CRC patients with high SPOCK1 expression had shorter OS, indicating that SPOCK1 played an adverse role in clinical outcomes (Fig. 3G). Thus, the phenotype of SPOCK1 + fibroblasts in CRC was further investigated in the GSE205506 dataset. We collected proteins that participated in tumor immunity, chemotaxis, vascular and tissue remodeling, apoptosis, and autophagy from the OLINK immuno-oncology assay [31]. Compared to SPOCK1- fibroblasts, LGALS1, TGFB1, and CCL2 were observed to have higher expression in SPOCK1 + fibroblasts, suggesting their roles in immune suppression and facilitating tumor progression (Fig. 3H) [26, 32, 33]. Analysis of DEGs showed that the expression of THBS2, FAP, and SFRP2 was higher in SPOCK1 + fibroblasts, contributing to tumor aggressiveness and immune-exclusive TME (Fig. 3I) [12, 34, 35]. Subsequently, we conducted pathway analysis (Fig. 3J). Enhanced EMT pathway, promoting tumor metastasis, was found in SPOCK1 + fibroblasts. TNFα signaling via NF-κB and hypoxia pathways, involved in tumor progression, had more enrichment in SPOCK1 + fibroblasts. Alterations in glycolysis and kras signaling pathways in SPOCK1 + fibroblasts, were noted. Moreover, CRC patients with high SPOCK1 expression showed enhanced activities of EMT, oncogenic, and TGFβ signaling pathways at the bulk transcriptomics level (Fig. S4E). To further explore the effects of SPOCK1 on TME in CRC, we collected TME subtypes defined by Bagaev et al.: immune-enriched, fibrotic (IE/F); immune-enriched, nonfibrotic (IE); fibrotic (F); and immune-depleted (D) [36]. We noticed that SPOCK1 had active expression in the F and IE/F subtypes, which were characterized by enhanced TGFβ signaling pathway, abundant fibroblast infiltration and a high ratio of M2/M1 macrophages (Fig. 3K).

The co-location of MARCO + macrophages and SPOCK1 + fibroblasts worsened the clinical outcome of CRC patients

To confirm the close proximity of MARCO + macrophages and SPOCK1 + fibroblasts, we first assessed the correlation between MARCO and SPOCK1, which reached 0.732 at the bulk transcriptomics level (Fig. 4A). At the single-cell level, the correlation between the abundance of MARCO + macrophages and SPOCK1 + fibroblasts was 0.858 (Fig. S5A). In the ST data, a congruous distribution pattern of MARCO and SPOCK1 was observed in the tumor region of P1, verifying the co-localization of MARCO + macrophages and SPOCK1 + fibroblasts (Fig. 4B; Fig. S5B). In addition, MIF analysis performed on 30 CRC samples confirmed the co-location of MARCO + macrophages and SPOCK1 + fibroblasts at the protein level (Fig. 4C).

We further explored the clinical significance of MARCO + macrophages and SPOCK1 + fibroblasts. In the bulk transcriptomics data, CRC patients with high expression of both MARCO and SPOCK1 had the shortest OS, suggesting the potential interplay between them that played a pro-tumor role (Fig. 4D). We then divided CRC patients into early stage (I or II) and late stage (III or IV) based on TNM stage. In the bulk transcriptomics data, SPOCK1 showed higher expression in CRC patients with late stage, while there was no difference in MARCO expression (Fig. 4E). Both expression of MARCO in macrophages and SPOCK1 in fibroblasts was higher in CRC patients with late stage in the single-cell dataset GSE132465 (Fig. 4F). In terms of consensus molecular subtypes (CMSs) for CRC, the expression of MARCO in macrophages and SPOCK1 in fibroblasts was higher in CMS1 and CMS4 samples in the single-cell dataset GSE132465 (Fig. 4G). CMS1 patients featured worse survival after relapse while CMS4 patients had worse OS and relapse-free survival (RFS) [37]. Subsequently, TIDE algorithm was used to predict the immunotherapy response of CRC patients in the bulk transcriptomics data. Compared to responders (R), both MARCO and SPOCK1 exhibited higher expression in non-responder (NR) CRC patients (Fig. 4H). Besides, the expression of MARCO and SPOCK1 both had positive correlations with TIDE scores (Fig. 4I). In the single-cell dataset GSE205506, MARCO displayed higher expression in macrophages from CRC patients with non-pCR after immunotherapy than in those with pCR (Fig. 4J). Due to the number of fibroblasts being too small in CRC patients with non-pCR in the GSE205506 dataset, it was hard to compare the expression of SPOCK1 in fibroblasts from CRC patients

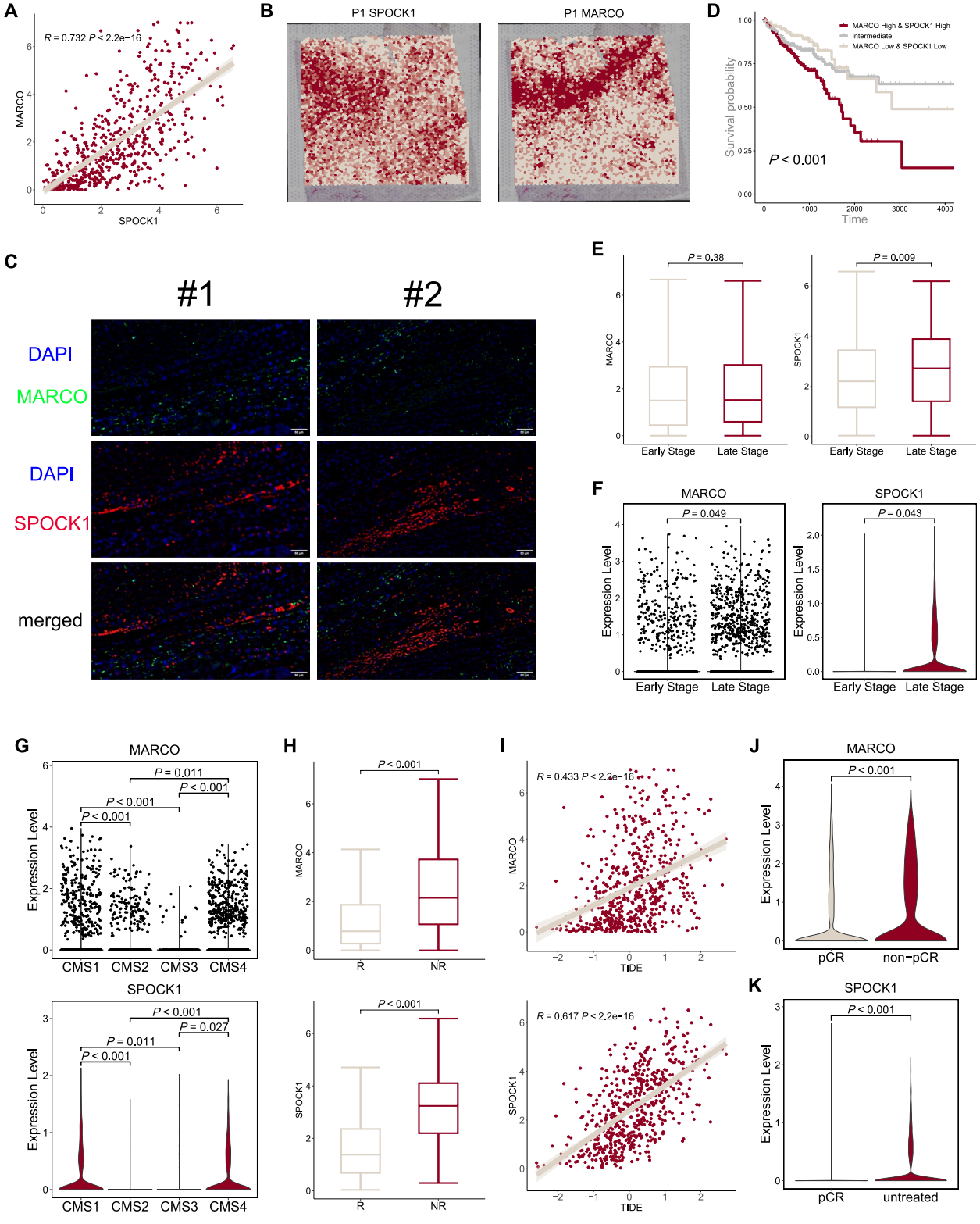

Fig. 4 (See legend on next page.)

(See figure on previous page.)

Fig. 4 The co-location of MARCO + macrophages and SPOCK1 + fibroblasts worsened the clinical outcome of colorectal cancer (CRC) patients. **A** The correlation between MARCO and SPOCK1 in the bulk transcriptomics data. **B** The distribution of MARCO and SPOCK1 in P1 in the spatial transcriptomics (ST) data. **C** The multiplex immunofluorescence (MIF) performed on 30 CRC patients exhibited the co-location between MARCO and SPOCK1. **D** CRC patients with both high MARCO and high SPOCK1 expression had worst prognosis in the bulk transcriptomics data. **E** The differences in MARCO and SPOCK1 expression between early and advanced stage CRC patients in the bulk transcriptomics data. **F** The differences in the expression of MARCO in macrophages and SPOCK1 in fibroblasts between early and advanced stage CRC patients in the single-cell dataset GSE205506. **G** The differences in the expression of MARCO in macrophages and SPOCK1 in fibroblasts among four consensus molecular subtypes (CMSs) in the single-cell dataset GSE132465. **H** The differences in MARCO and SPOCK1 expression between responders (R) and non-responders (NR) predicted by the TIDE algorithm in the bulk transcriptomics data. **I** The MARCO and SPOCK1 expression both showed positive correlations with TIDE scores in the bulk transcriptomics data. **J** The difference in MARCO expression in macrophages between pathological complete response (pCR) and non-pCR CRC patients after immunotherapy in the single-cell dataset GSE205506. **K** The difference in SPOCK1 expression in fibroblasts between CRC patients with pCR after immunotherapy and those without immunotherapy at the single-cell level

with non-pCR and pCR. Thus, we combined fibroblasts in the GSE205506 and GSE132465 datasets to explore the difference in the expression of SPOCK1 in fibroblasts from CRC patients with pCR after immunotherapy and those untreated with immunotherapy. Compared to CRC patients with pCR after immunotherapy, the expression of SPOCK1 was higher in fibroblasts from CRC patients without immunotherapy (Fig. 4K).

Cell–cell communication involved in MARCO + macrophages and SPOCK1 + fibroblasts

To further understand the roles of MARCO + macrophages and SPOCK1 + fibroblasts in the TME of CRC, we investigated their communication networks in the single-cell dataset GSE205506. Before that, inferCNV analysis was conducted to identify malignant cells from epithelial cells (Fig. S6). The cell–cell communication analysis revealed that MARCO + macrophages had stronger interactions with other cell types compared to MARCO- macrophages, especially with SPOCK1 + fibroblasts (Fig. 5A). Additionally, SPOCK1 + fibroblasts showed enhanced interplay with other cell types than SPOCK1- fibroblasts, especially with MARCO + macrophages (Fig. 5B). These findings suggested that MARCO + macrophages and SPOCK1 + fibroblasts influenced each other, exerting a collaborative impact on tumor progression and immunosuppressive TME. Thus, we then explored the crosstalk among MARCO + macrophages, SPOCK1 + fibroblasts, malignant cells, and T cells. We noticed that various signaling pathways, mainly associated with proliferation and immunity, were activated among the above four cell types, in which MARCO + macrophages and SPOCK1 + fibroblasts were the primary senders (Fig. 5C). SPP1, EGF, and COMPLEMENT signaling pathways were the main interactions between MARCO + macrophages and SPOCK1 + fibroblasts. Specifically, SPP1 and HBEGF, which played roles in promoting proliferation, released from MARCO + macrophages interacted with the corresponding receptors on SPOCK1 + fibroblasts (Fig. 5D and F). C3, involved in regulating M2 polarization, released from SPOCK1 + fibroblasts interacted with C3AR1, ITGAX, ITGB2, and ITGAM on MARCO + macrophages (Fig. 5E) [38]. As for malignant cells, HBEGF, linked to cell growth, released from MARCO + macrophages interacted with ERBB2, ERBB4, and EGFR on malignant cells (Fig. 5F). Besides, SPOCK1 + fibroblasts might facilitate malignant cell proliferation via PTN and WNT signaling pathways (Fig. 5G). In terms of T cells, MARCO + macrophages mainly interacted with T cells via the ligand LGALS9, which was associated with suppressed antitumor immunity (Fig. 5H) [39]. Moreover, CXCL12 released from SPOCK1 + fibroblasts interacted with CXCR4 on T cells. There was evidence that the CXCL12-CXCR4 axis functioned to inhibit the infiltration of cytotoxic T cells (Fig. 5I) [40].

Discussion

Despite the remarkable success of immunotherapy in tumor treatment, only a small portion of CRC patients respond to this therapy, highlighting the necessity of investigating the underlying mechanisms of immune resistance. Macrophages are key TME components regulating tumor immunity [5]. The intratumor macrophage infiltration has great heterogeneity and complex interactions with other cells, which remain incompletely characterized. Our study revealed two intratumor macrophage infiltration patterns, macrophage + and macrophage-, in CRC samples at the ST level. MARCO + macrophages accumulated in the macrophage + sample, co-localizing with SPOCK1 + fibroblasts. The presence of MARCO + macrophages and SPOCK1 + fibroblasts shaped an immunosuppressive TME, which induced to the poor prognosis and inferior immunotherapy response. Since MARCO + macrophages highly express SPP1 and SPOCK1 + fibroblasts highly express FAP, our findings align with and extend those of Qi et al. [12].

The intratumor accumulation of MARCO + macrophages were observed in the macrophage + sample in our study. We found that MARCO + macrophages were M2 macrophages with immunosuppressive properties and were associated with poor prognosis in CRC, consistent with the findings from recent research clarifying the role of MARCO + macrophages in intrahepatic cholangiocarcinoma [41]. In the B16 melanoma model, MARCO

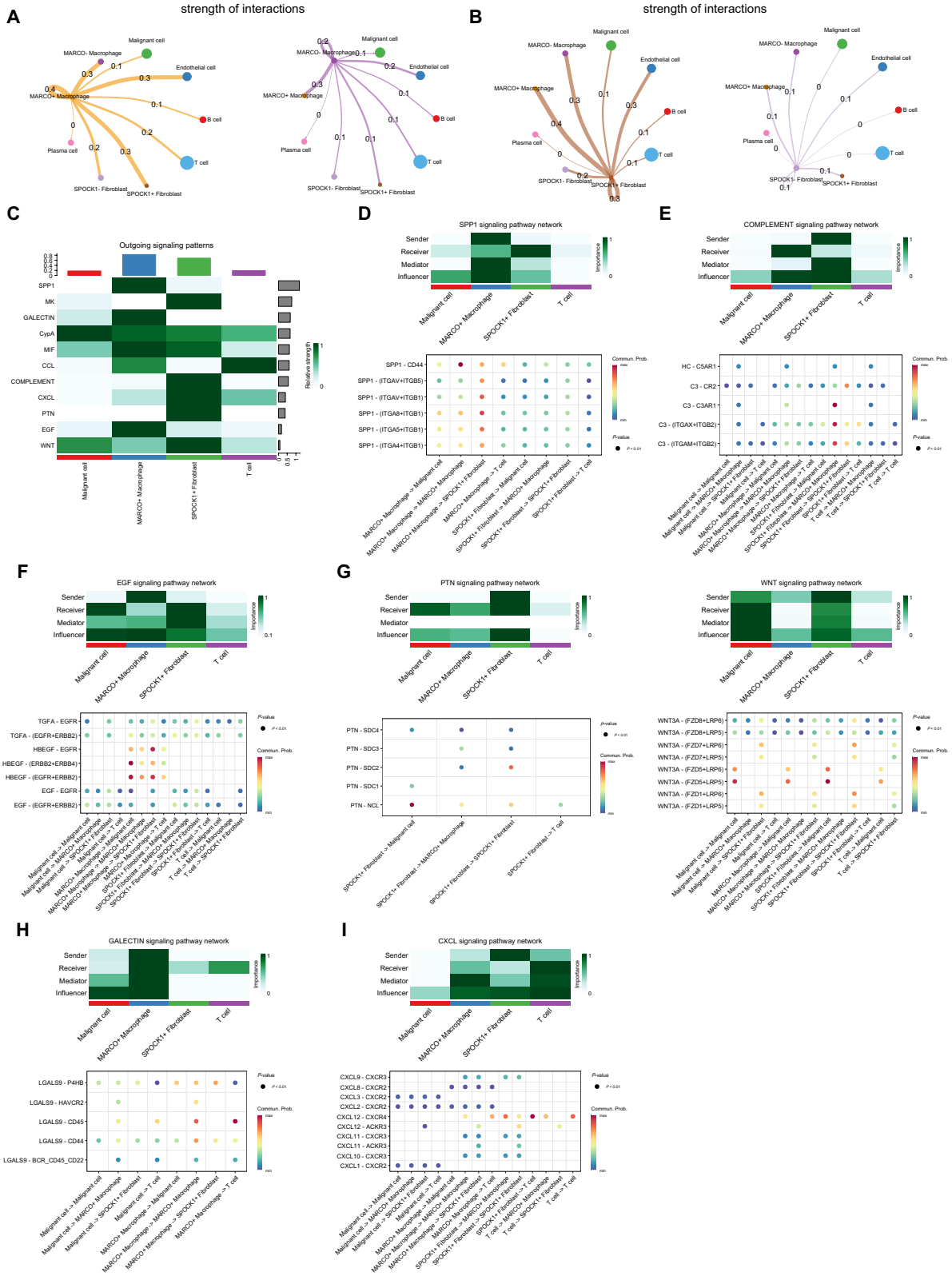

Fig. 5 Cell–cell communication involved in MARCO + macrophages and SPOCK1 + fibroblasts. **A** The difference in interaction strengths between MARCO + macrophages and MARCO- macrophages with other cell types. **B** The difference in interaction strengths between SPOCK1 + fibroblasts and SPOCK1 - fibroblasts with other cell types. **C** The outgoing pattern of all cell clusters. **D** The SPP1 signaling pathway network. **E** The COMPLEMENT signaling pathway network. **F** The EGF signaling pathway network. **G** The PTN and WNT signaling pathway network. **H** The GALECTIN signaling pathway network. **I** The CXCL signaling pathway network

monoclonal antibodies promote a shift in the polarization of MARCO-expressing macrophages from M2 to M1 [42]. In addition, macrophages from CRC patients with non-pCR after anti-PD-1 therapy showed higher MARCO expression compared to those with pCR, suggesting that high infiltration of MARCO macrophages predicted worse immunotherapy response. It has been reported that anti-PD-L1 resistance in hepatocellular carcinoma can be improved by MARCO + macrophage-targeted treatment [43]. In melanoma, anti-MARCO antibody treatment contributes to the activation of NK cells, enhancing the tumor killing effects of immunotherapy, including antibodies to PD-1 or PD-L1 [44]. We also identified LGALS9 as a key ligand by which MARCO + macrophages may suppress T cells. In gastric cancer, C1Q + macrophages suppressed the activation and promoted the exhaustion of GZMA + T lymphocytes, potentially through the LGALS9-CD45 axis [45]. High expression of LGALS9 is associated with poor prognosis in distinct cancer types and anti-tumor immunity can be boosted by targeting LGALS9 [46]. Furthermore, MARCO + macrophages appeared to promote malignant cell proliferation via EGF signaling. Taken together, MARCO is a promising target to overcome immune suppression and enhance immunotherapy sensitivity and effectiveness in CRC.

SPOCK1 + fibroblasts were found to be co-localized with MARCO + macrophages in the macrophage + sample. We noticed that SPOCK1 + fibroblasts contributed to the immunosuppressive TME and were linked to poor prognosis in CRC. There is evidence that SPOCK1 is a risk factor for prognosis in certain cancer types [47–49]. In lung adenocarcinoma, high expression of SPOCK1 correlates with low infiltration of CD8 + T cells, contributing to immune escape [48]. Moreover, TIDE algorithm showed that SPOCK1 was a potential regulator of immunotherapy response in CRC. Fibroblasts from CRC patients with pCR after anti-PD-1 therapy had lower expression of SPOCK1 compared to those who were untreated. The unfavorable role of SPOCK1 + fibroblasts in immunotherapy might be partially explained by the finding that SPOCK1 + fibroblasts interacted with T cells through the CXCL12-CXCR4 axis, which inhibits the differentiation of CD8 + naïve T cells into CD8 + cytotoxic T lymphocytes, weakening anti-tumor activity [40]. Besides, SPOCK1 + fibroblasts promote malignant cell proliferation via PTN and WNT signaling pathways. In summary, SPOCK1 serves as a potential target in CRC treatment.

The intercellular interplay between MARCO + macrophages and SPOCK1 + fibroblasts was further investigated. The crosstalk between these cells involved MARCO + macrophages secreting SPP1 and HBEGF to stimulate SPOCK1 + fibroblast proliferation, while SPOCK1 + fibroblasts secreted C3, potentially reinforcing M2 polarization of macrophages via the C3-C3AR1 axis, which activates PI3Kγ signaling [38]. This reciprocal interaction creates a synergistic immunosuppressive niche. Hence, therapeutic strategies targeting MARCO + macrophages, SPOCK1 + fibroblasts, or their crosstalk could reshape the immunosuppressive TME, improving the response and efficacy of immunotherapies in CRC.

Some limitations still remains in our study. A larger number of ST samples is necessary to further confirm the spatial patterns described. The close proximity of MARCO + macrophages and SPOCK1 + fibroblasts in the MIF needs to be quantitatively analyzed. In vivo and in vitro experiments are needed to verify the interactions between MARCO + macrophages and SPOCK1 + fibroblasts and to further explore the mechanisms of the immunosuppressive roles of MARCO + macrophages and SPOCK1 + fibroblasts. Meanwhile, the clinical significance of MARCO + macrophages and SPOCK1 + fibroblasts, particularly regarding immunotherapy response, requires validation in larger, dedicated immunotherapy cohorts and prospective studies.

Conclusion

Our study delineates the intratumor macrophage infiltration patterns in CRC and identifies the co-location of MARCO + macrophages and SPOCK1 + fibroblasts as a key feature of the immunosuppressive TME. These findings provide insights into novel therapeutic avenue targeting MARCO + macrophages, SPOCK1 + fibroblasts, or their crosstalk for CRC patients.

Abbreviations

CRC	Colorectal cancer
MSI-H	High microsatellite instability
TME	Tumor microenvironment
TAMs	Tumor-associated macrophages
ST	Spatial transcriptomics
MIF	Multiplex immunofluorescence
GEO	Gene Expression Omnibus
pCR	Pathological complete response
TCGA	The Cancer Genome Atlas
FFPE	Formalin-fixed paraffin-embedded
DEGs	Differentially expressed genes
GSEA	Gene set enrichment analysis
TSA	Tyramide signal amplification
KM	Kaplan–Meier
TIDE	The tumor immune dysfunction and exclusion
CNVs	Copy number variations
OS	Overall survival
EMT	Epithelial mesenchymal transition
CMSs	Consensus molecular subtypes
RFS	Relapse-free survival

Supplementary Information

The online version contains supplementary material available at https://doi.org/10.1186/s12885-025-15397-x.

Supplementary Material 1.

Acknowledgements
Thanking the online databases contributing to this work and all researchers who provided publicly available datasets analyzed in this work.

Authors' contributions
PYH: Writing-original draft, Methodology, Investigation, Visualization, Formal analysis, Data curation, Conceptualization. YH: Writing-review & editing, Software, Resources. LMY: Visualization, Validation. XQJ: Writing-review & editing, Supervision, Conceptualization. All authors contributed to the article and approved the submitted version.

Funding
This research was supported by Zhejiang Clinovation Pride(CXTD202501028) and General Research Project (Natural Science Category) of Zhejiang Provincial Department of Education (Grant No.Y202558353).

Data availability
The data used in this article are available in the TCGA database (https://portal.gdc.cancer.gov/) and the GEO database (https://www.ncbi.nlm.nih.gov/geo/).

Declarations

Ethics approval and consent to participate
The study was approved by the Ethics Committee of the Fourth Affiliated Hospital of School of Medicine, Zhejiang University (No: K2025019) and was in compliance with the Declaration of Helsinki. Informed written consent from all patients involved was obtained.

Consent for publication
Not applicable.

Competing interests
The authors declare no competing interests.

Received: 27 June 2025 / Accepted: 26 November 2025
Published online: 28 November 2025

References

1. Bray F, Laversanne M, Sung H, Ferlay J, Siegel RL, Soerjomataram I, et al. Global cancer statistics 2022: GLOBOCAN estimates of incidence and mortality worldwide for 36 cancers in 185 countries. CA Cancer J Clin. 2024;74(3):229–63.
2. Ganesh K, Stadler ZK, Cercek A, Mendelsohn RB, Shia J, Segal NH, et al. Immunotherapy in colorectal cancer: rationale, challenges and potential. Nat Rev Gastroenterol Hepatol. 2019;16(6):361–75.
3. Zaanan A, Shi Q, Taieb J, Alberts SR, Meyers JP, Smyrk TC, et al. Role of deficient DNA mismatch repair status in patients with stage iii colon cancer treated with FOLFOX adjuvant chemotherapy: a pooled analysis from 2 randomized clinical trials. JAMA Oncol. 2018;4(3):379–83.
4. Nordholm-Carstensen A, Krarup PM, Morton D, Harling H, Danish Colorectal Cancer Group. Mismatch repair status and synchronous metastases in colorectal cancer: A nationwide cohort study. Int J Cancer. 2015;137(9):2139–48.
5. DeNardo DG, Ruffell B. Macrophages as regulators of tumour immunity and immunotherapy. Nat Rev Immunol. 2019;19(6):369–82.
6. Yang D, Yang L, Cai J, Hu X, Li H, Zhang X, et al. A sweet spot for macrophages: focusing on polarization. Pharmacol Res. 2021;167:105576.
7. Shapouri-Moghaddam A, Mohammadian S, Vazini H, Taghadosi M, Esmaeili SA, Mardani F, et al. Macrophage plasticity, polarization, and function in health and disease. J Cell Physiol. 2018;233(9):6425–40.
8. Pittet MJ, Michielin O, Migliorini D. Clinical relevance of tumour-associated macrophages. Nat Rev Clin Oncol. 2022;19(6):402–21.
9. Yang X, Deng B, Zhao W, Guo Y, Wan Y, Wu Z, et al. FABP5+ lipid-loaded macrophages process tumour-derived unsaturated fatty acid signal to suppress T-cell antitumour immunity. J Hepatol. 2025;82(4):676–89.
10. Schaer DJ, Schulthess-Lutz N, Baselgia L, Hansen K, Buzzi RM, Humar R, et al. Hemorrhage-activated NRF2 in tumor-associated macrophages drives cancer growth, invasion, and immunotherapy resistance. J Clin Invest. 2023;134(3):e174528.
11. Lee SH, Lee D, Choi J, Oh HJ, Ham IH, Ryu D, et al. Spatial dissection of tumour microenvironments in gastric cancers reveals the immunosuppressive crosstalk between CCL2+ fibroblasts and STAT3-activated macrophages. Gut. 2024;3:gutjnl-2024-332901.
12. Qi J, Sun H, Zhang Y, Wang Z, Xun Z, Li Z, et al. Single-cell and spatial analysis reveal interaction of FAP+ fibroblasts and SPP1+ macrophages in colorectal cancer. Nat Commun. 2022;13(1):1742.
13. Nazemalhosseini-Mojarad E, Mohammadpour S, Torshizi Esafahani A, Gharib E, Larki P, Moradi A, et al. Intratumoral infiltrating lymphocytes correlate with improved survival in colorectal cancer patients: independent of oncogenetic features. J Cell Physiol. 2019;234(4):4768–77.
14. Backman M, Strell C, Lindberg A, Mattsson JSM, Elfving H, Brunnström H, et al. Spatial immunophenotyping of the tumour microenvironment in non-small cell lung cancer. Eur J Cancer. 2023;185:40–52.
15. Jovic D, Liang X, Zeng H, Lin L, Xu F, Luo Y. Single-cell RNA sequencing technologies and applications: a brief overview. Clin Transl Med. 2022;12(3):e694.
16. Mei Y, Xiao W, Hu H, Lu G, Chen L, Sun Z, et al. Single-cell analyses reveal suppressive tumor microenvironment of human colorectal cancer. Clin Transl Med. 2021;11(6):e422.
17. Vickovic S, Eraslan G, Salmén F, Klughammer J, Stenbeck L, Schapiro D, et al. High-definition spatial transcriptomics for in situ tissue profiling. Nat Methods. 2019;16(10):987–90.
18. Sibai M, Cervilla S, Grases D, Musulen E, Lazcano R, Mo CK, et al. The spatial landscape of cancer hallmarks reveals patterns of tumor ecological dynamics and drug sensitivity. Cell Rep. 2025;44(2):115229.
19. Li J, Wu C, Hu H, Qin G, Wu X, Bai F, et al. Remodeling of the immune and stromal cell compartment by PD-1 blockade in mismatch repair-deficient colorectal cancer. Cancer Cell. 2023;41(6):1152-1169.e7.
20. Lee HO, Hong Y, Etlioglu HE, Cho YB, Pomella V, Van den Bosch B, et al. Lineage-dependent gene expression programs influence the immune landscape of colorectal cancer. Nat Genet. 2020;52(6):594–603.
21. Ru B, Huang J, Zhang Y, Aldape K, Jiang P. Estimation of cell lineages in tumors from spatial transcriptomics data. Nat Commun. 2023;14(1):568.
22. Jiang P, Gu S, Pan D, Fu J, Sahu A, Hu X, et al. Signatures of T cell dysfunction and exclusion predict cancer immunotherapy response. Nat Med. 2018;24(10):1550–8.
23. Goswami KK, Bose A, Baral R. Macrophages in tumor: an inflammatory perspective. Clin Immunol. 2021;232:108875.
24. Jia Y, Zhang B, Zhang C, Kwong DLW, Chang Z, Li S, et al. Single-cell transcriptomic analysis of primary and metastatic tumor ecosystems in esophageal squamous cell carcinoma. Adv Sci (Weinh). 2023;10(7):e2204565.
25. Cheng S, Li Z, Gao R, Xing B, Gao Y, Yang Y, et al. A pan-cancer single-cell transcriptional atlas of tumor infiltrating myeloid cells. Cell. 2021;184(3):792-809.e23.
26. Nixon BG, Gao S, Wang X, Li MO. TGFβ control of immune responses in cancer: a holistic immuno-oncology perspective. Nat Rev Immunol. 2023;23(6):346–62.
27. Zhao B, Li H, Xia Y, Wang Y, Wang Y, Shi Y, et al. Immune checkpoint of B7–H3 in cancer: from immunology to clinical immunotherapy. J Hematol Oncol. 2022;15(1):153.
28. Zhang Y, Chen H, Mo H, Zhao N, Sun X, Liu B, et al. Distinct cellular mechanisms underlie chemotherapies and PD-L1 blockade combinations in triple-negative breast cancer. Cancer Cell. 2025;43(3):446-463.e7.
29. Grasmann G, Smolle E, Olschewski H, Leithner K. Gluconeogenesis in cancer cells - Repurposing of a starvation-induced metabolic pathway? Biochimica et Biophysica Acta (BBA). 2019;1872(1):24–36.
30. de Visser KE, Joyce JA. The evolving tumor microenvironment: from cancer initiation to metastatic outgrowth. Cancer Cell. 2023;41(3):374–403.
31. Kartsonaki C, Pang Y, Millwood I, Yang L, Guo Y, Walters R, et al. Circulating proteins and risk of pancreatic cancer: a case-subcohort study among Chinese adults. Int J Epidemiol. 2022;51(3):817–29.
32. Chen Q, Han B, Meng X, Duan C, Yang C, Wu Z, et al. Immunogenomic analysis reveals LGALS1 contributes to the immune heterogeneity and immunosuppression in glioma. Int J Cancer. 2019;145(2):517–30.
33. Xu M, Wang Y, Xia R, Wei Y, Wei X. Role of the CCL2-CCR2 signalling axis in cancer: mechanisms and therapeutic targeting. Cell Prolif. 2021;54(10):e13115.
34. Yang H, Sun B, Fan L, Ma W, Xu K, Hall SRR, et al. Multi-scale integrative analyses identify THBS2+ cancer-associated fibroblasts as a key orchestrator promoting aggressiveness in early-stage lung adenocarcinoma. Theranostics. 2022;12(7):3104–30.

35. Wang Q, Zhao Y, Tan G, Ai J. Single cell analysis revealed SFRP2 cancer associated fibroblasts drive tumorigenesis in head and neck squamous cell carcinoma. NPJ Precis Oncol. 2024;8(1):228.
36. Bagaev A, Kotlov N, Nomie K, Svekolkin V, Gafurov A, Isaeva O, et al. Conserved pan-cancer microenvironment subtypes predict response to immunotherapy. Cancer Cell. 2021;39(6):845-865.e7.
37. Guinney J, Dienstmann R, Wang X, de Reyniès A, Schlicker A, Soneson C, et al. The consensus molecular subtypes of colorectal cancer. Nat Med. 2015;21(11):1350–6.
38. Zha H, Wang X, Zhu Y, Chen D, Han X, Yang F, et al. Intracellular activation of complement C3 leads to PD-L1 antibody treatment resistance by modulating tumor-associated macrophages. Cancer Immunol Res. 2019;7(2):193–207.
39. Mariño KV, Cagnoni AJ, Croci DO, Rabinovich GA. Targeting galectin-driven regulatory circuits in cancer and fibrosis. Nat Rev Drug Discov. 2023;22(4):295–316.
40. Lu Y, Liu Y, Zuo X, Li G, Wang J, Liu J, et al. CXCL12+ tumor-associated endothelial cells promote immune resistance in hepatocellular carcinoma. J Hepatol. 2025;82(4):634–48.
41. Fan G, Tao C, Li L, Xie T, Tang L, Han X, et al. The co-location of MARCO+ tumor-associated macrophages and CTSE+ tumor cells determined the poor prognosis in intrahepatic cholangiocarcinoma. Hepatology. 2024;82(1):25–41.
42. Georgoudaki AM, Prokopec KE, Boura VF, Hellqvist E, Sohn S, Östling J, et al. Reprogramming tumor-associated macrophages by antibody targeting inhibits cancer progression and metastasis. Cell Rep. 2016;15(9):2000–11.
43. Ding L, Qian J, Yu X, Wu Q, Mao J, Liu X, et al. Blocking MARCO+ tumor-associated macrophages improves anti-PD-L1 therapy of hepatocellular carcinoma by promoting the activation of STING-IFN type I pathway. Cancer Lett. 2024;1(582):216568.
44. Eisinger S, Sarhan D, Boura VF, Ibarlucea-Benitez I, Tyystjärvi S, Oliynyk G, et al. Targeting a scavenger receptor on tumor-associated macrophages activates tumor cell killing by natural killer cells. Proc Natl Acad Sci U S A. 2020;117(50):32005–16.
45. Peng H, Jiang L, Yuan J, Wu X, Chen N, Liu D, et al. Single-cell characterization of differentiation trajectories and drug resistance features in gastric cancer with peritoneal metastasis. Clin Transl Med. 2024;14(10):e70054.
46. Yang R, Sun L, Li CF, Wang YH, Yao J, Li H, et al. Galectin-9 interacts with PD-1 and TIM-3 to regulate T cell death and is a target for cancer immunotherapy. Nat Commun. 2021;12(1):832.
47. Zheng H, Liu H, Li H, Dou W, Wang X. Weighted gene co-expression network analysis identifies a cancer-associated fibroblast signature for predicting prognosis and therapeutic responses in gastric cancer. Front Mol Biosci. 2021;8:744677.
48. Liu Y, Han T, Wu J, Zhou J, Guo J, Miao R, et al. SPOCK1, as a potential prognostic and therapeutic biomarker for lung adenocarcinoma, is associated with epithelial-mesenchymal transition and immune evasion. J Transl Med. 2023;21(1):909.
49. Lin YW, Wen YC, Hsiao CH, Lai FR, Yang SF, Yang YC, et al. Proteoglycan SPOCK1 as a poor prognostic marker promotes malignant progression of clear cell renal cell carcinoma via triggering the snail/Slug-MMP-2 axis-mediated epithelial-to-mesenchymal transition. Cells. 2023;12(3):352.

Publisher's Note